PAPER

Check for updates

A promising TNT alternative 3,3′-bi(1,2,4-oxadiazole)-5,5′-diylbis(methylene)dinitrate (BOM): thermal behaviors and eutectic characteristics

Xiong Yang,[a] Jing Zhou,[a] Xiaoling Xing,[a] Yafeng Huang,[a] Zhengfeng Yan,[a] Qi Xue,[a] Xiaofeng Wang*[a] and Bozhou Wang [ID] *[ab]

3,3′-Bi(1,2,4-oxadiazole)-5,5′-diylbis(methylene)dinitrate (BOM) is a liquid phase carrier for melt cast explosives that is expected to replace TNT. The combination of a conjugated 1,2,4-oxadiazole backbone and nitrate ester groups endows BOM with both good energetic performance and impressive insensitivity. In this paper, the thermal behaviors of BOM were investigated using a TG–DSC synchronous thermal analyzer, proving that BOM is basically non-volatile under heating and melting processes. The apparent activation energy of BOM calculated by the Kissinger method was 158.2 kJ mol^{-1} at atmospheric pressure, which is higher than that of DNTF at atmospheric pressure and TNT at 2 MPa, indicating good thermal stability at low temperatures. The thermal decomposition mechanism of BOM was studied through both DSC-MS and *in situ* FTIR technologies. The low eutectic characteristics of BOM and DNTF were also investigated carefully and the best ratio of BOM/DNTF was 40/60 with a melting point at 75.5 °C. Finally, the detonation performances of TNT/HMX, BOM/HMX and BOM/DNTF(40/60)/HMX explosive formulations were calculated, showing that the detonation performances of the latter two formulations were significantly higher than that of TNT/HMX.

Introduction

Pursuing high energy and insensitivity is the eternal goal in the field of explosives.[1] The melt cast explosives are mixed energetic systems in which solid-phase particles of high-energy explosives are added to a molten liquid carrier matrix explosive to form a flow for casting,[2] which is one of the main charge methods of the current warheads. 2,4,6-Trinitrotoluene (TNT) has low production costs and high safety, which makes it the most important carrier applied for melt cast explosives. Despite all that, there are some fateful shortcomings of TNT when applied in the formation of melt cast explosives, including the high vapor pressure, high toxicity,[3] serious environmental pollution,[4] and poor detonation performance. Therefore, intensive studies have been carried out towards the development of new alternatives to replace TNT during the past few decades. 2,4-Dinitroanisole (DNAN),[5] 1,3,3-trinitroazetidine (TNAZ)[6] and 3,4-dinitrofurazanfuroxan (DNTF)[7] are reported potential alternatives to TNT; however, all of them suffer from some insuperable problems, such as high volatility, mechanical sensitivity and melting point. The main properties of most currently used or studied liquid phase carriers for melt cast explosives are summarized in Table 1.[8]

BOM is a newly discovered liquid carrier for melt cast explosives. As shown in Fig. 1, the structure of BOM successfully combines a conjugated isofurazan backbone with oxidative nitrate ester groups, achieving both good energetic performance and impressive insensitivity. A preliminary study showed that the melting point of BOM is only 85.8 °C, while the

Table 1 The main properties of liquid phase carriers for melt cast explosives

Exp	MP, °C	ρ, g cm^{-3}	D, km s^{-1}	P, GPa	S_i, H_{50}, cm	S_f
BOM	85.8	1.823	8.18	28.1	8.6 J	282 N
TNT	80.8	1.64	6.94	21	$H_{50} = 79$	4–6%
DNAN	94.5	1.34	5.60	7.02	$H_{50} = 220$	170 N
TNAZ	101	1.84	8.73	37.2	$H_{50} = 21$	353 N
DNTF	110	1.937	9.25	41.1	$H_{50} = 20$	84%
MTNI	82	1.78	8.80	35.5	$H_{50} = 100$	252 N
DNP	86	1.81	8.24	28.8	—	—
MDNT	98	1.676	7.66	—	$H_{50} = 100$	252 N
MTNP	91	1.83	8.96	33.5	—	—
DNBF	85	1.85	8.80	35.6	$H_{50} = 12$	—
ADN	92	1.82	—	—	$H_{50} = 24$	72%
DINA	51.3	1.488	7.58	28.6	—	—
NG-N1	66	1.799	8.84	32.6	14 J	96 N
TNE	86	1.92	9.1	40	2.7 J	75 N
TTA	94	1.54	5.68	—	—	—

[a]Xi'an Modern Chemistry Research Institute, Xi'an, 710065, China. E-mail: wbz600@163.com; wangxf_204@163.com

[b]State Key Laboratory of Fluorine & Nitrogen Chemical, Xi'an, 710065, China
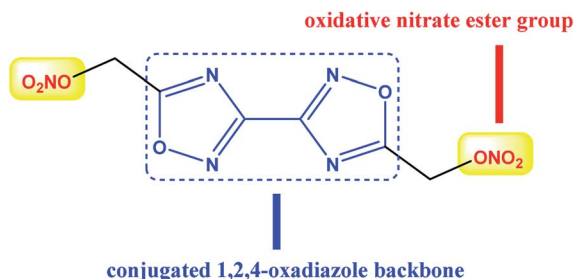
Fig. 1 The molecular structure of BOM.

thermal decomposition temperature reaches 200 °C, showing attractive application prospects as a carrier for melt cast explosives. The energy level of BOM is about 1.5 times the TNT equivalent with a density of 1.823 g cm^{-3} and a detonation velocity of 8180 m s^{-1}. With an impact sensitivity of 8.6 J and a friction sensitivity of 282 N, the safety performance of BOM is even better than that of RDX. Moreover, BOM has also been proved as an environmentally-friendly explosive molecule.[9] All of these make BOM an ideal alternative to TNT.

As a potential carrier for melt cast explosives, systematic studies on the thermal behaviors and decompositions of BOM are important for its future applications. Herein, we report studies on the thermal behavior, thermal decomposition kinetic parameters and thermal decomposition mechanism of BOM. In terms of application, the development of eutectics is an effective means to improve the performance of melt cast explosive carriers. In order to increase the energy level of BOM, the eutectic characteristics of BOM and DNTF were also studied, and the phase diagram was drawn to determine the optimal ratio of the two. In addition, the detonation performance parameters of BOM/HMX and BOM/DNTF(40/60)eutectic/HMX were estimated, and the effect of BOM instead of TNT was evaluated from the perspective of detonation performance.

Experiment

Reagents and sample preparation

(1) BOM[10] (99.0%) and DNTF[11] (99.0%) were supplied by Xi'an Modern Chemistry Research Institute. The synthesis of BOM was performed according to the literature, including the cyclization, hydrolysis and nitration procedures (Fig. 2).

(2) To test the low eutectic properties, 0.1 g BOM/DNTF mixtures with different proportions (100/0, 90/10, 80/20, 70/
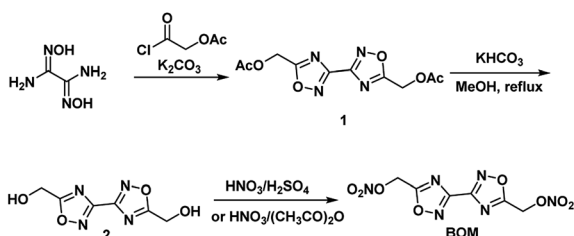
30, 60/40, 50/50, 40/60, 30/70, 20/80, 10/90, 0/100) were prepared, added to 10 mL of acetone for dissolution, and left still until the solvent volatilized completely to obtain a crystal mixture of BOM and DNTF. The crystal mixture (1.0 mg) was heated to 115 °C in a DSC instrument, cooled immediately after the crystal mixture was completely melted, and then heated to 120 °C. The DSC curves were obtained, and the binary phase diagram of BOM/DNTF was drawn according to the DSC curves.

Apparatus and measurements

The thermal analysis experiments were performed on a model TG–DSC STA449C instrument (NETZSCH, Germany). Operation conditions: sample mass, 1.03 mg; atmosphere, dynamic nitrogen; aluminum cell.

In situ FTIR spectroscopy was carried out on a Nexus 870 FTIR spectrometer. Operation conditions: sample mass, 1.08 mg; heating rate, 10 °C min^{-1}; resolution, 4 cm^{-1}; spectral acquisition rate, 7.5 file min^{-1}, 8 scans·file^{-1}; temperature range, 25–465 °C.

The mass spectra (MS) were obtained with a QMS403 Four Bar Mass Spectrometer. Test quality range, 1–300 amu; resolution < 0.5 amu; detection limit > 1 ppm.

Results and discussion

Thermal behaviors of BOM

A TG–DSC synchronous thermal analyzer was used to study the thermal decomposition behaviors of BOM. The heating rate was 5 °C min^{-1}, and the TG–DSC curves are shown in Fig. 3.

It can be seen from Fig. 3 that there is an endothermic peak and an exothermic peak in the heating process of BOM. The endothermic peak is the melting endothermic peak of BOM, which is at the temperature of 85.8 °C, and the exothermic peak is the decomposition exothermic peak of BOM at 203.4 °C. For most liquid-phase carriers of melt cast explosives, their melting points are at between 70 and 120 °C. An ideal melting point is below 100 °C, since the molding and processing process of energetic materials can be completed by using the temperature condition of steam. The melting endothermic peak of BOM is at
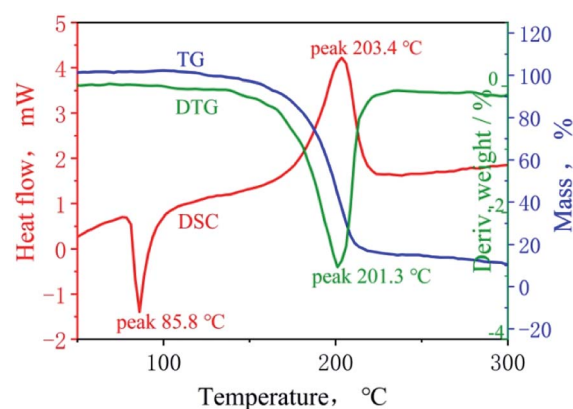

Fig. 2 The synthesis of BOM.
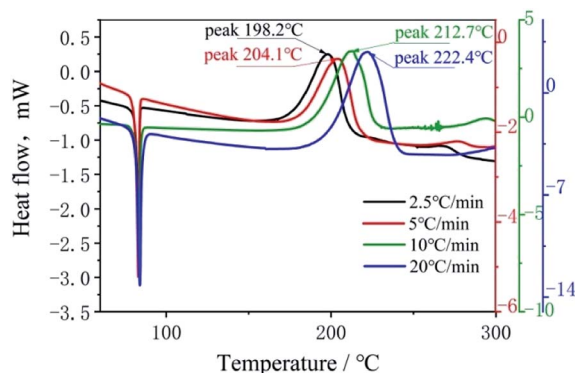

Fig. 3 TG–DSC curves of BOM.

Fig. 4 DSC curves of BOM at different heating rates.

Table 2 Kinetic parameters for the thermal decomposition reaction of BOM

β_i, K min^{-1}	T_i, K	E_k, kJ mol^{-1}	r	lg A_k, s^{-1}
2.5	471.0	158.2	0.9848	19.55
5	477.1			
10	486.1			
20	495.3			

85.8 °C. This shows that BOM is very suitable to be used as an explosives carrier.

In the TG curve, the weight of BOM decreased rapidly at 201.3 °C, and the weight loss was close to 70%, which was the main stage of thermal decomposition.

The decomposition peak in the DSC curve of BOM is almost the same as that corresponding to the peak of DTG, indicating that BOM was hard to volatilize before the thermal decomposition. Unlike other volatile melt cast explosive carriers, especially TNT, non-volatility is another good characteristic of BOM. It is not harmful to the human respiratory system or eyes during the operation process.

Thermal decomposition kinetic parameters of BOM

In order to investigate the thermal stability and the non-isothermal kinetics of thermal decomposition of BOM, DSC curves at different heating rates were employed (Fig. 4). The heating rates were 2.5 °C min^{-1}, 5.0 °C min^{-1}, 10.0 °C min^{-1} and 20.0 °C min^{-1}, respectively.

The Kissinger model[12] was used to calculate the kinetic parameters (apparent activation energy (E_k) and pre-exponential constant (A_k)) of the decomposition reaction of BOM. The Kissinger model can be expressed as follows:

$$\ln\left(\frac{\beta_i}{T_i^2}\right) = -\frac{E_k}{R} \times \frac{1}{T_i} + \ln\left(\frac{A_k R}{E_k}\right) \quad (i = 1 - 4) \qquad (1)$$

where β_i is the heating rate, E_k is the apparent activation energy (kJ mol^{-1}), R is the gas constant (8.314 J K^{-1} mol^{-1}), A_k is the pre-exponential factor (s^{-1}), and T_i is the peak temperature (K).

The kinetic parameters for BOM obtained by the Kissinger model are given in Table 2.

In order to further investigate the thermal stability of BOM, the kinetic parameters of BOM, DNTF[13] at atmospheric pressure and TNT[14] at 2 MPa pressure obtained based on the Kissinger

Table 3 Kinetic parameters of BOM, DNTF and TNT

Exp	T, °C	T, K	1000, T	E_k, kJ mol^{-1}	E_k/RT	lg A_k, s^{-1}	K, s^{-1}
BOM 0.1 MPa	50	323.2	3.0941	158.2	58.8560	19.55	$10^{-6.01}$
	80	353.2	2.8313	158.2	53.8583	19.55	$10^{-3.84}$
	130	403.2	2.4802	158.2	47.1811	19.55	$10^{-0.94}$
	180	453.2	2.2065	158.2	41.9769	19.55	$10^{1.32}$
	230	503.2	1.9873	158.2	37.8068	19.55	$10^{3.13}$
	260	533.2	1.8755	158.2	35.6800	19.55	$10^{4.05}$
	300	573.2	1.7446	158.2	33.1906	19.55	$10^{5.13}$
	350	623.2	1.6046	158.2	30.5281	19.55	$10^{6.29}$
DNTF 0.1 MPa	50	323.2	3.0941	58.8	21.8825	7.76	$10^{-1.74}$
	80	353.2	2.8313	58.8	20.0238	7.76	$10^{-0.93}$
	130	403.2	2.4802	58.8	17.5407	7.76	$10^{0.15}$
	180	453.2	2.2065	58.8	15.6055	7.76	$10^{0.99}$
	230	503.2	1.9873	58.8	14.0549	7.76	$10^{1.66}$
	260	533.2	1.8755	58.8	13.2641	7.76	$10^{2.00}$
	300	573.2	1.7446	58.8	12.3385	7.76	$10^{2.41}$
	350	623.2	1.6046	58.8	11.3485	7.76	$10^{2.84}$
TNT 2 MPa	50	323.2	3.0941	110.9	41.2587	7.60	$10^{-10.3}$
	80	353.2	2.8313	110.9	37.7553	7.60	$10^{-8.79}$
	130	403.2	2.4802	110.9	33.0745	7.60	$10^{-6.76}$
	180	453.2	2.2065	110.9	29.4263	7.60	$10^{-5.18}$
	230	503.2	1.9873	110.9	26.5029	7.60	$10^{-3.91}$
	260	533.2	1.8755	110.9	25.0121	7.60	$10^{-3.26}$
	300	573.2	1.7446	110.9	23.2669	7.60	$10^{-2.50}$
	350	623.2	1.6046	110.9	21.4005	7.60	$10^{-1.69}$

method are shown in Table 3. The reaction rate constants are calculated and compared.

The decomposition peak temperatures of BOM at different heating rates are 198.2 °C, 204.1 °C, 212.7 °C and 222.4 °C, respectively. The apparent activation energy is 158.2 kJ mol^{-1}, which is much higher than that of DNTF (58.8 kJ mol^{-1}) at atmospheric pressure, and that of TNT (110.93 kJ mol^{-1}) at 2 MPa. This indicates that BOM has good thermal stability at low temperature. The reaction rate constant of BOM is greater than that of TNT at 2 MPa, but much less than that of DNTF at atmospheric pressure.

The thermal decomposition mechanism of BOM

The thermal decomposition of BOM was determined by MS and *in situ* FTIR. MS can be used to detect the ion fragments in the process of sample heating and decomposition, and *in situ* FTIR can be used to detect the characteristic infrared spectra of intermediate products and final products in the process of heating and decomposition.

MS can detect the thermal decomposition ion fragments of BOM in real time, and the relation curves between the detected main ion fragment currents and temperature are shown in Fig. 5.

It can be seen from the mass spectrogram that a NO ($m/z = 30$) fragment was detected at 100 °C, which indicates that a small amount of nitro and nitroso were transformed into each other in the process of denitrification of BOM, and a small amount of NO was first decomposed and released.[15] When the temperature reached 140 °C, small amounts of 1,2,4-oxadiazole ring ($m/z = 68$) and $\cdot CH_2–O–O\cdot$ ($m/z = 46$) were formed. When the temperature was increased to 170 °C, a large number of ion fragments with $m/z = 30$, 46 and 68 were formed rapidly, especially those with $m/z = 30$. It is speculated that the separation of $–NO_2$ groups ($m/z = 46$) should start at this time, with the separation of $\cdot CH_2–O\cdot$ ($m/z = 30$) and the 1,2,4-oxadiazole ring ($m/z = 68$) from the BOM structure at the same time. When the temperature is higher than 170 °C, NO_2 will decompose immediately to NO ($m/z = 30$). The ion fragment with $m/z = 30$ contains $\cdot CH_2–O\cdot$ and NO, so the amount of formation is very
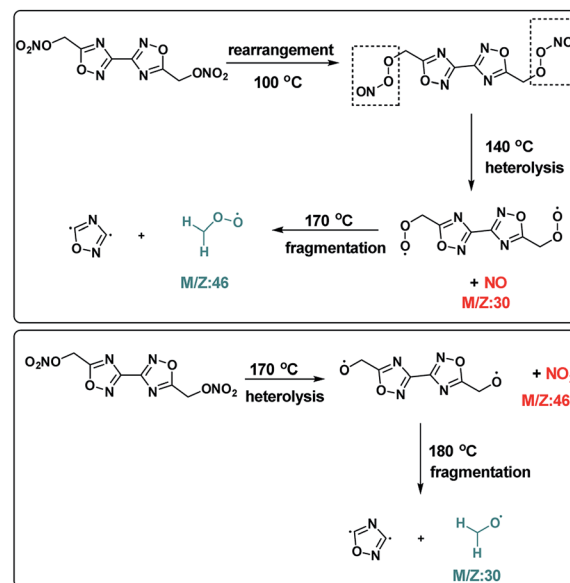

Fig. 6 The thermal decomposition process of BOM.

large. When the temperature reached 180 °C, ion fragments with $m/z = 12$, 18, 26 and 44 were detected, which were considered as the final product fragments of the plasma fragments of $\cdot CH_2–O\cdot$ and the 1,2,4-oxadiazole ring, respectively, C, H_2O, $\cdot CN$ and CO_2. Therefore, this suggested that the BOM thermal decomposition process is as shown in Fig. 6.[16]

In situ FTIR technology can detect the infrared spectrum of the remaining condensed matter in BOM from the beginning of heating to the end of decomposition. The infrared spectra at 40 °C, 100 °C, 170 °C, 200 °C and 220 °C during heating are shown in Fig. 7.

At 40 °C, the peaks at 3000 cm^{-1}, 2952 cm^{-1} and 2924 cm^{-1} are the characteristic peaks of methylene ($–CH_2–$), and those at 1660 cm^{-1}, 1288 cm^{-1} and 848 cm^{-1} are the antisymmetric stretching vibration peak, symmetric stretching vibration peak and N–O stretching vibration peak of the oxidative nitrate ester
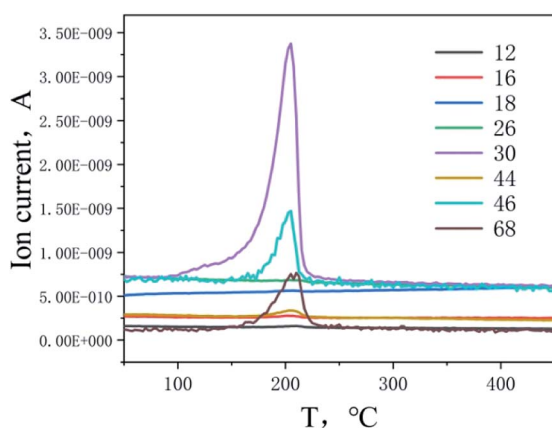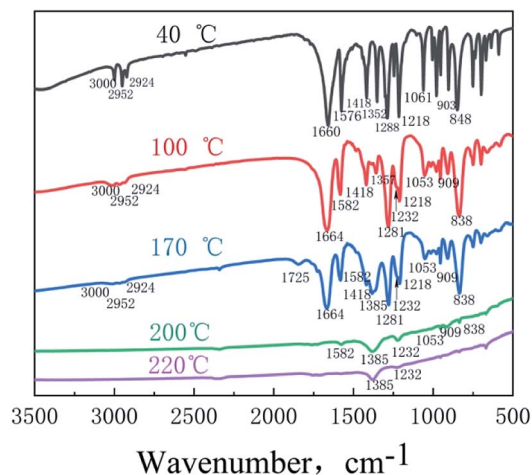

Fig. 5 MS spectra of BOM products.
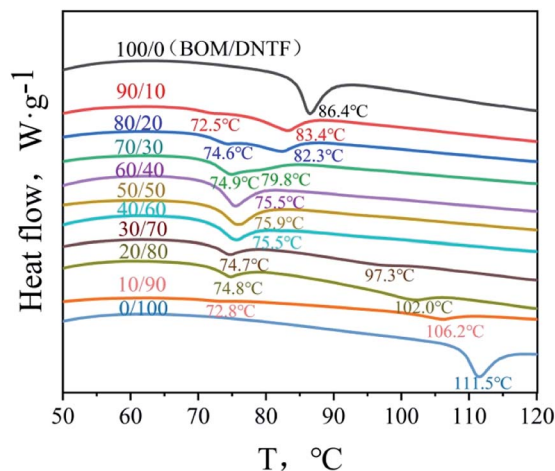

Fig. 7 The infrared spectra at 40, 100, 170, 200 and 220 °C.

Paper

Fig. 8 DSC curves of BOM/DNTF in different proportions.

Fig. 9 Binary phase diagram of BOM/DNTF.

group (–ONO$_2$), respectively.[17] In addition, the peaks at 1576 cm^{-1}, 1418 cm^{-1}, 1352 cm^{-1}, 1061 cm^{-1} and 903 cm^{-1} are the characteristic peaks of 1,2,4-oxadiazole.[18]

With an increase in temperature, BOM melted completely at 100 °C (from DSC, the melting temperature of BOM is 85.8 °C). At this time, the infrared characteristic peak of liquid BOM has different degrees of deviation compared with that of solid BOM: 1660→1664 cm^{-1}, 1576→1582 cm^{-1}, 1352→1357 cm^{-1}, 1288→1281 cm^{-1}, 1061→1053 cm^{-1}, 903→909 cm^{-1}, 848→838 cm^{-1}, etc. This shows that the change of BOM state has some influence on the position of its infrared characteristic peaks. At 100 °C, a peak at 1232 cm^{-1} appeared which is the characteristic peak of nitrite. It is speculated that NO and H$_2$O in the air react with KBr tablets in the in situ cell to generate KNO$_2$, which also proves that a small amount of nitro and nitroso transform into each other first in mass spectrometry at 100 °C, and a small amount of NO is released first.

When the temperature rises to about 170 °C, new peaks at 1385 cm^{-1} and 1725 cm^{-1} appear in the infrared spectrum, which are the characteristic peaks of nitrate and carbonyl. The peak at 1725 cm^{-1} is very weak, but that at 1385 cm^{-1} becomes stronger and stronger with the increase of temperature. This shows that when the temperature is about 170 °C, the nitrate
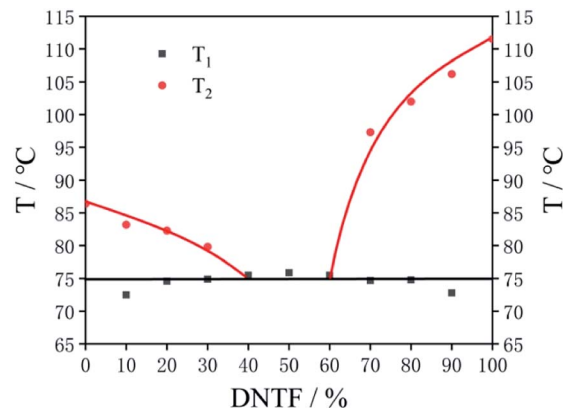
group of BOM begins to denitrify and catalyzes the loss of a H from a small amount of methylene,[19] forming a carbonyl. NO$_2$ and H$_2$O in the air react with KBr tablets in the in situ cell to form KNO$_3$. When heated to about 200 °C, denitration is completed and the characteristic peaks of the nitrate ester group disappear completely. Only the characteristic peaks of carbonyl, 1,2,4-oxadiazole ring, KNO$_2$ and KNO$_3$ are left in the spectrum.

When the temperature increases to about 220 °C, the 1,2,4-oxadiazole ring in the pool is completely cracked, and the characteristic peaks disappeared. Finally, only the characteristic peaks of KNO$_2$ (1232 cm^{-1}) and KNO$_3$ (1385 cm^{-1}) are left.

The low eutectic characteristic of BOM and DNTF

Deep eutectic solvents (DESs) are newly discovered green solvents, which have found a very wide spectrum of use, such as absorption, extraction and catalysis.[20] DESs are composed of two or more compounds via hydrogen bonding interactions between hydrogen-bond donors and hydrogen-bond acceptors. DESs are liquid around room temperature because they have a lower melting point than either of the individual components.[21]

Table 4 Melting points of BOM/DNTF in different proportions

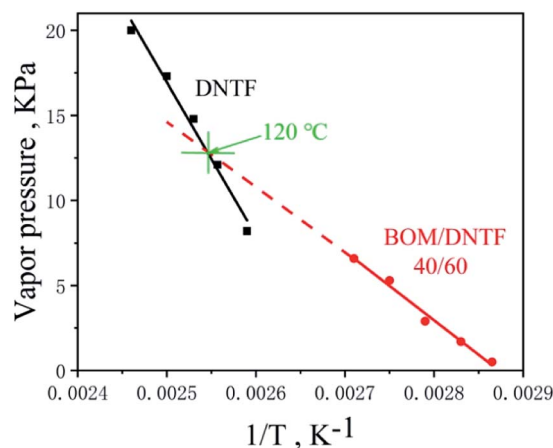| BOM/DNTF	T_1, °C	T_2, °C
100/0	—	86.4
90/10	72.5	83.2
80/20	74.6	82.3
70/30	74.9	79.8
60/40	75.5	—
50/50	75.9	—
40/60	75.5	—
30/70	74.7	97.3
20/80	74.8	102.0
10/90	72.8	106.2
0/100	—	111.5

Fig. 10 Temperature dependence of vapor pressure for DNTF and the BOM/DNTF(40/60) low eutectic.

Table 5 The impact, friction and ESD sensitivity of DNTF, BOM and BOM/DNTF (40/60)

Exp	Impact, H_{50}, cm	Friction, %	ESD
DNTF	20.0	84	No initiation
BOM	115.3	22	No initiation
BOM/DNTF(40/60)	106.8	24	No initiation

Similar to the deep eutectic solvents, researchers often melt and mix two kinds of melt cast explosive carriers to obtain a low melting point liquid phase carrier in the field of melt cast explosives, which is called a low eutectic. The preparation of a low eutectic is an effective way to improve the performance of fused cast explosive carriers. DNTF[22] has the advantages of high energy, high detonation velocity and high density, but its sensitivity is high, and its melting point is 108 °C, which is not conducive to steam forming. The advantages of BOM are high density, low melting point and low sensitivity, but the detonation performance of BOM is lower than that of DNTF. If DNTF and BOM can form a low melting point eutectic, the safety and high melting point of DNTF will be improved significantly, and the detonation performance of BOM will be improved at the same time.[23] Therefore, in this chapter, the melting points of BOM/DNTF at different proportions (100/0, 90/10, 80/20, 70/30, 60/40, 50/50, 40/60, 30/70, 20/80, 10/90, 0/100) are tested by DSC (Fig. 8), and the low eutectic characteristics of BOM and DNTF

are studied. Table 4 shows the melting points of BOM/DNTF at different proportions, T_1 is the first endothermic peak temperature, and T_2 is the second endothermic peak temperature.

The binary phase diagram of BOM/DNTF is obtained by the T–Z (temperature–composition) method from the data in Table 4 (Fig. 9). It can be seen from the phase diagram that when the ratio of BOM/DNTF is 60/40, 50/50 and 40/60, they formed a complete eutectic with melting points of 75.5 °C, 75.9 °C and 75.5 °C, respectively.

The ideal melting temperature of a melt cast explosive carrier should be between 70 and 120 °C. If the melting point is lower than 100 °C, it is more conducive to steam melt processing. The melting points of the BOM/DNTF low eutectics with the proportions of 60/40, 50/50 and 40/60 are very ideal, and suitable for use as the carrier of melt cast explosives. Considering that the detonation performance of DNTF is better than that of BOM, it is considered that the 40/60 BOM/DNTF low eutectic has the best detonation performance, and 40% BOM will greatly reduce the sensitivity of the system. Table 5 shows the results of impact, friction and ESD sensitivity tests. The impact sensitivity was investigated using the drop height of 50% explosion probability (H_{50}) with the drop weight of 5 kg. The friction sensitivity was tested by the method of explosion probability (conditions: the mass of the pendulum was 1.5 kg and the swing angle was 90°). The ESD test was carried out by charging a capacitor of 10 000 pF to 10 kV, and testing the samples 30 times under four conditions (0.12 mm/0 Ω, 0.25 mm/0 Ω, 0.18 mm/100 kΩ and 0.50 mm/100 kΩ) to observe the reaction of the explosives.

Table 6 Detonation performance parameters of melt cast explosives carriers

Sample	Density, g cm^{-3}	OB, %	Detonation heat, J g^{-1}	Detonation velocity, m s^{-1}	Detonation pressure, GPa
TNT	1.654	−73.96	4380.45	6809.01	18.70
BOM	1.823	−33.32	4857.29	8092.01	28.11
BOM/DNTF(40/60)	1.931	−18.90	6008.45	9079.33	37.87
BOM/DNTF(50/50)	1.917	−21.31	5815.85	8919.67	36.18
BOM/DNTF(60/40)	1.899	−23.71	5620.03	8749.84	34.32

Table 7 Detonation performance parameters of melt cast explosive systems

Sample	Density, g cm^{-3}	OB, %	Detonation heat, J g^{-1}	Detonation velocity, m s^{-1}	Detonation pressure, GPa
TNT/HMX	1.796	−42.55	5174.33	8194.57	28.72
BOM/HMX	1.871	−26.29	5347.88	8712.74	33.78
BOM/DNTF(40/60)/HMX	1.915	−20.53	5797.43	9041.98	37.11
BOM/DNTF(50/50)/HMX	1.887	−21.49	5777.20	8996.10	36.93
BOM/DNTF(60/40)/HMX	1.879	−22.45	5700.71	8934.18	36.28

From the test results, 40% BOM can effectively reduce the impact sensitivity and friction sensitivity of DNTF. DNTF, BOM and BOM/DNTF (40/60) are insensitive to electric sparks because they are not initiated under ESD test conditions.

The vapor pressure of a melt cast explosive liquid carrier is a performance metric that we are very concerned about. Therefore, we tested the vapor pressures of DNTF and the BOM/DNTF(40/60) low eutectic with increasing temperatures, and compared their volatility at their use temperatures. The results are shown in Fig. 10.

It can be seen from Fig. 10 that the BOM/DNTF(40/60) low eutectic has lower vapor pressure values at its actual use temperature (melting point to 20 °C above the melting point), lower than that of DNTF. The vapor pressure value of the low eutectic increases slowly with the increase of temperature, and the rate is lower than that of DNTF. Linear fitting of the measured data shows that the vapor pressure curves of the two carriers have a cross point at 120 °C.

To evaluate the detonation performance of the low eutectic, the detonation properties of TNT, BOM and the BOM/DNTF (40/60) low eutectic were calculated by EXPLO5 software.[24] The results are shown in Table 6.

It can be seen from Table 6 that the detonation performance of BOM is better than that of TNT in all aspects. BOM and DNTF are prepared into a low eutectic with a percentage of 40/60. The detonation performance is greatly improved compared with BOM, with a density of 1.931 g cm^{-3}, detonation heat of 6008.45 J g^{-1}, detonation velocity of 9079.33 m s^{-1} and detonation pressure of 37.87 GPa.

Prediction of the detonation performance

In view of improving the detonation performance, when the carrier explosive has high detonation performance, a high melting point explosive with excellent detonation performance should be chosen as the solid component of the melt cast explosives. HMX is a kind of explosive with comprehensive properties.[25] As a solid component, it is very beneficial to improve the detonation performance of melt cast explosives.

According to the charge characteristics of melt cast explosives, the carrier content of the liquid phase is generally set at 40%, and the solid component content of high energy is set at 60%. In order to investigate the detonation properties of the melt cast explosives with BOM or BOM/DNTF as liquid phase carriers and HMX as a high-energy solid-phase explosive component, the detonation parameters of TNT/HMX, BOM/HMX and BOM/DNTF (40/60)/HMX were calculated by EXPLO5 software (Table 7). Fig. 11 is obtained by drawing the data in Table 5.

The results show that the detonation parameters of the melt cast explosives with BOM and BOM/DNTF (40/60) as liquid carriers are significantly higher than that of TNT. The explosion heat, detonation velocity and detonation pressure of BOM/HMX are 5347.88 J g^{-1}, 8712.74 m s^{-1} and 33.78 GPa, respectively, and are 3.4%, 6.3% and 17.6% higher than those of TNT/HMX. The detonation heat, detonation velocity and detonation pressure of BOM/DNTF(40/60)/HMX are 5797.43 J g^{-1},
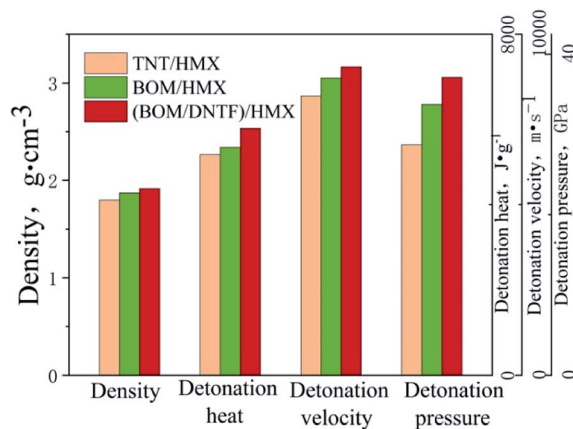

Fig. 11 Comparison of detonation performance.

9041.98 m s^{-1} and 37.11 GPa, respectively, 8.4%, 3.8% and 11.8% higher than those of BOM/HMX, and 12.0%, 10.4% and 29.2% higher than those of TNT/HMX.

Therefore, from the perspective of detonation performance, BOM and BOM/DNTF (40/60) can replace TNT as the liquid phase carrier of high-energy melt cast explosives.

Conclusions

BOM is a newly discovered liquid carrier of melt cast explosives with high energy and low sensitivity, which has potential application prospects in the field of high energy melt cast explosives. In this paper, the thermal decomposition behavior and mechanism of BOM, as well as the characteristics and detonation properties of the low eutectic with DNTF, were studied and the main conclusions are as follows:

(1) From the TG–DSC, when the heating rate is 5 °C min^{-1}, the melting peak of BOM is 85.8 °C, and the decomposition peak is 203.4 °C, so it is basically non-volatile before decomposition.

(2) The apparent activation energy of BOM obtained by the Kissinger method is 158.2 kJ mol^{-1}, which is much higher than that of DNTF at atmospheric pressure (58.8 kJ mol^{-1}), and that of TNT at 2 MPa (110.93 kJ mol^{-1}). This shows that BOM has good thermal stability at low temperature.

(3) In the decomposition process of BOM, a small amount of nitro and nitroso are transformed into each other first, then nitro is separated, the 1,2,4-oxadiazole ring and branch chain are separated, and finally the 1,2,4-oxadiazole ring is completely decomposed.

(4) BOM/DNTF with the proportions of 60/40, 50/50 and 40/60 can form a complete low eutectic. The analysis shows that the comprehensive performance of BOM/DNTF with the proportion of 40/60 is the best.

(5) When the composition of liquid-phase carrier and solid-phase high-energy explosive (HMX) is 40%/60%, the detonation performance is calculated by EXPLO5 as follows: the detonation heat, detonation velocity and detonation pressure of BOM/HMX are 5347.88 J g^{-1}, 8712.74 m s^{-1} and 33.78 GPa, respectively, 3.4%, 6.3% and 17.6% higher than those of TNT/HMX. The

detonation heat, detonation velocity and detonation pressure of BOM/DNTF(40/60)/HMX are 5797.43 J g^{-1}, 9041.98 m s^{-1} and 37.11 GPa, respectively, 8.4%, 3.8% and 11.8% higher than those of BOM/HMX, and 12.0%, 10.4% and 29.2% higher than those of TNT/HMX.

Based on the above research content and results, it is considered that BOM has low sensitivity, is nontoxic, and has excellent detonation performance, and is therefore very suitable as a liquid-phase carrier of melt cast explosives. It has huge application prospects, and is expected to replace TNT in an all-round way after its mass production.

Conflicts of interest

There are no conflicts to declare.

Acknowledgements

Notes and references

1 M. Lu, *Chin. J. Energ. Mater.*, 2018, **26**, 373; P. C. Zhang, X. X. Zhao, Y. Du, M. Govin, S. H. Li and S. P. Pang, *RSC Adv.*, 2018, **8**, 24627; T. L. Zhang, C. H. Lu, J. G. Zhang and K. B. Yu, *Propellants, Explos., Pyrotech.*, 2003, **28**, 271; J. G. Zhang, T. L. Zhang, Z. G. Zhang and L. Yang, *Chin. J. Energ. Mater.*, 2001, **9**, 90.

2 P. Ravi, D. M. Badgujar, G. M. Gore, S. P. Tewari and A. K. Sikder, *Propellants, Explos., Pyrotech.*, 2011, **36**, 393; Q. H. Wang, *Chin. J. Explos. Propellants*, 2011, **34**, 25.

3 B. S. Levine, E. M. Furedi, D. E. Gordon, J. J. Barkley and P. M. Lish, *Toxicol. Sci.*, 1990, **15**, 373.

4 Y. G. Wu, D. W. Zhao, C. H. Zhao and L. Hui, *Chin. J. Explos. Propellants*, 2004, **27**, 42.

5 P. Samuels, *Insensitive Munitions and Energetic Materials, IMEM Symposium*, 2012, vol. 14.

6 Q. L. Jiang, H. Wang, Y. M. Luo, W. Wang, H. X. Wang, J. Gao and K. Zhao, *Initiators Pyrotech.*, 2014, **3**, 42; J. Z. Li, X. Z. Fan and B. Z. Wang, *Chin. J. Energ. Mater.*, 2004, **12**, 305.

7 W. Zheng and J. N. Wang, *Chin. J. Energ. Mater.*, 2006, **14**, 463.

8 P. Ravi, D. M. Badgujar, G. M. Gore, S. P. Tewari and A. K. Sikder, *Propellants, Explos., Pyrotech.*, 2011, **36**, 393; D. L. Cao, Y. J. Li, Y. Du, J. L. Wang and Y. X. Li, *Chin. J. Energ. Mater.*, 2013, **21**, 157; Q. H. Wang, *Chin. J. Explos. Propellants*, 2011, **34**, 25; S. Du, J. L. Zhao, Y. X. Li, J. L. Wang and D. L. Cao, *Chem. Intermed.*, 2011, **6**, 532; X. M. Zhang, H. S. Dong, J. Sun, D. Y. Gao, Y. X. Xia, X. F. Liu and X. Dong, *Chin. J. Energ. Mater.*, 2012, **20**, 555; P. Liu, N. X. Xu and C. M. Ying, *Chin. J. Explos. Propellants*, 1999, **2**, 19; W. Zhang, W. X. Xie, X. Z. Fan, F. L. Liu, W. Q. Pang, X. G. Liu and Y. P. Ji, *Chin. J. Explos. Propellants*, 2015, **2**, 81; D. E. Chavez, M. A. Hiskey, D. L. Naud and D. Parrish, *Angew. Chem.*, 2008, **120**, 8307; A. Thomas, A. Penger and M. K. Thomas, *Cent. Eur. J.*

Energ. Mater., 2009, **6**, 255; N. Sikder, A. K. Sikder, N. R. Bulakh and B. R. Candhe, *J. Hazard. Mater.*, 2004, **113**, 35.

9 E. C. Johnson, J. J. Sabatini, D. E. Chavez, R. C. Sausa, E. F. C. Byrd, L. A. Wingard and P. E. Guzman, *Org. Process Res. Dev.*, 2018, **22**, 736; R. C. Sausa, I. G. Batyrev, R. A. Pesce-Rodriguez and E. F. C. Byrd, *J. Phys. Chem. A*, 2018, **122**, 9043.

10 Q. Xue, F. Q. BI, Y. S. Zhou, M. J. Wu, H. Huo, J. R. Zhang, Y. F. Luo, L. J. Zhai, S. Y. Zhang and B. Z. Wang, *Chin. J. Explos. Propellants*, 2019, **42**, 236.

11 Y. S. Zhou, B. Z. Wang, J. k. Li, H. C. Zhou, L. Hu, Z. Q. Chen and Z. Z. Zhang, *Acta Chim. Sin.*, 2011, **69**, 1673.

12 J. Zhou, L. Ding, F. Q. Bi, B. Z. Wang and J. L. Zhang, *J. Anal. Appl. Pyrolysis*, 2018, **129**, 189; J. Y. Lee, M. J. Shim and S. W Kim, *J. Appl. Polym. Sci.*, 2001, **81**, 479; C. Nikovia, A. P. Maroudas, P. Goulis, D. Tzimis, P. Paraskevopoulou and M. Pitsikalis, *Molecules*, 2015, **20**, 15597.

13 X. N. REN, J. N. Wang, C. P. Yin, H. J. Wei, S. Y. Heng and P. Yue, *Chin. J. Explos. Propellants*, 2006, **29**, 33.

14 H. Q. LI, C. W. An, M. Y. Du, X. M. Wen and J. Y. Wang, *Chin. J. Explos. Propellants*, 2016, **39**, 58.

15 R. S. Booth and L. J. Butler, *J. Chem. Phys.*, 2014, **141**, 134315; Q. B. Fu, Y. J. Shu and Y. G. Huang, *J. Solid Rocket Technol.*, 2010, **33**, 77; J. Kimura, *Propellants, Explos., Pyrotech.*, 1989, **14**, 89.

16 M. A. Hiskey, K. R. Brower and J. C. Oxley, *J. Phys. Chem. B*, 1991, **95**, 3955; J. B. Levy, *J. Am. Chem. Soc.*, 1954, **76**, 3790.

17 E. Pretsch, P. Buehlmann and C. Affolter, *Structure determination of organic compounds*, Springer-Verlag, 2000.

18 G. Socrates, *Infrared Characteristic Group Frequencies*, John Wiley & Sons, 1980.

19 H. Chang, *Initiators Pyrotech.*, 2007, **2**, 38.

20 Y. Chen, D. Yu, W. Chen, L. Fu and T. C. Mu, *Phys. Chem. Chem. Phys.*, 2019, **21**, 2601; P. Makoś, E. Słupek and J. Gębicki, *Microchem. J.*, 2019, **152**, 104384; I. D. Inaloo and S. Majnooni, *Chemistryselect*, 2019, **4**, 7811.

21 A. Pande, Bhawna, D. Dhingra and S. Pandey, *J. Phys. Chem. B*, 2017, **121**, 4202; A. Faraone, D. V. Wagel, G. A. Baker, E. C. Novak, M. Ohl, D. Reuter, P. Lunkenheimer, A. Loidl and E. Mamontov, *J. Phys. Chem. B*, 2018, **122**, 1261.

22 V. P. Sinditskii, A. V. Burzhava, A. B. Sheremetev and N. S. Aleksandrova, *Propellants, Explos., Pyrotech.*, 2012, **37**, 575; Q. H. Wang, *Chin. J. Explos. Propellants*, 2003, **26**, 13; F. Q. Zhao, P. Chen, R. Z. Hu, Y. Luo, Z. Z. Zhang, Y. S. Zhou, X. W. Yang, Y. Gao, S. L. Gao and Q. Z. Shi, *J. Hazard. Mater.*, 2004, **113**, 67.

23 Q. L. Jiang, H. Wang, Y. M. Luo, W. Wang, H. X. Wang and J. Gao, *Initiators Pyrotech.*, 2014, **0**, 42; Y. H. Shao, X. N. Ren, Z. R. Liu and X. Zhang, *J. Therm. Anal. Calorim.*, 2011, **103**, 617; N. Liu, S. Zeman, Y. J. Shu, Z. K. Wu, B. Z. Wang and S. W. Yin, *RSC Adv.*, 2016, **6**, 59141.

24 M. Suceska, *EXPLO5, version 6.04*, 2017.

25 W. C. Mcrone, *Anal. Chem.*, 1950, **22**, 1225; D. M. Badgujar, M. B. Talawar, S. N. Asthana and P. P. Mahulikar, *J. Hazard. Mater.*, 2008, **151**, 289; S. Xiong, S. Chen, S. Jin, Z. Zhang and L. Li, *RSC Adv.*, 2017, **7**, 6795.